2.1 CHARACTERIZATION OF A LARGER BEST PRACTICE HEAT OF 14YWT IN ANNEALED POWDER, HIP CONSOLIDATED AND EXTRUDED FORMS —

N. J. Cunningham, Y. Wu, G. R. Odette, (University of California, Santa Barbara); D. T. Hoelzer, (Oak Ridge National Laboratory); and S. A. Maloy (Los Alamos National Laboratory)

OBJECTIVES

The objective is to characterize a set of 14YWT alloys made from a large heat of gas atomized and mechanically alloyed powder using an alternative processing method that incorporates Y during the gas atomization process.

SUMMARY

We describe the characterization of new 14YWT heats from gas atomized and mechanically alloyed powder using an alternative processing method that incorporates Y during the gas atomization process. Post mechanically alloying processes included annealing the powder at 850ºC and 1150ºC, HIP consolidation at 850ºC and 1150ºC, and consolidation by hot extrusion at 850ºC, annealing for 1 h at 1000ºC, and then cross-rolling to 50% thickness at 1000ºC; the latter has been dubbed FCRD-NFA1. In all cases a high number density of nm-sized features were observed using a combination of atom probe tomography, transmission electron microscopy, and small angle neutron scattering. The 850ºC lower temperature annealing and HIP consolidation resulted in smaller precipitates compared to the 1150ºC processing temperature. However, after annealing at 1200ºC for 48 h the precipitate size and number density were similar in the two cases. The FCRD-NFA1 had a microstructure and NF distribution similar to a previously reported alloy, PM2. However, the extruded samples also had a large number of large (>20 nm) Ti-rich precipitates. These larger precipitates may affect the mechanical properties, which are currently under investigation.

BACKGROUND

Nanostructured ferritic alloys (NFAs) have outstanding properties for applications in advanced fission and fusion reactors. NFAs are strengthened and made irradiation tolerant by a high number density of thermally stable Y-Ti-O nanofeatures (NFs). The conventional NFA processing path uses ball milling to mechanically alloy Y_2O_3 in the Fe-Cr matrix, which is an expensive process and often leads to heterogeneous distributions of NFs. To overcome these challenges an alternative processing path in which Y is included in the melt prior to gas atomization and rapid solidification was developed in collaboration with partner institutions including Oak Ridge National and Los Alamos National Laboratory, ATI Powder Metals, UC Berkeley and South Dakota School of Mines. Many small lab heats of NFA were prepared using this alternative processing method and analyzed in a program primarily funded by the DOE Office of Nuclear Energy [1]. The results of this extensive effort were used to identify the best processing practices. A previous report detailed the production, characterization, and mechanical property testing of the final extruded and hot cross-rolled heat known as 14YWT-PM2 (PM2) for the small-batch studies [2]. This report describes a larger heat of gas atomized and ball milled powder that was produced using the “best practices” knowledge gained by the smaller scale testing.

ATI Powder Metals Laboratory (Pittsburgh, PA) produced the 14YWT-atomized powders in its Laboratory Gas Atomizer (LGA) vacuum induction melting (VIM) furnace. Details of the atomization process are described elsewhere [2]. After atomization the Y is phase separated

and requires ball milling. A total of 15 kg of nominal 14wt.%Cr-3wt.%W-0.35wt.%Ti-0.25wt.%Y iron alloy powder was ball milled by Zoz, GmbH (Wenden, Germany) with 52.5 g of FeO powder for 40 h in a CM100b attritor mill with a ball mass-to-charge ratio of 10:1 and ball size of 5 mm. The canister was evacuated and backfilled with Ar three times to remove any atmosphere contamination and milled in Ar at an overpressure of 100 mbar. The milling speed alternated between 256 (2 minutes) and 150 rpm (10 minutes). FeO was added to increase the O content to ≈ 0.08 wt.%.

This milled powder (V540) was analyzed in several conditions, including as annealed powder, after HIP consolidation and after hot extrusion. After outgassing at 400ºC under vacuum the powder was annealed at both 850 and 1150ºC for 3 h at 15ºC/min ramp and cooling rates. Atom probe tomography (APT) was performed on both conditions and TEM was performed on the 1150ºC-annealed powder. Two HIP consolidated alloys were produced from the outgassed samples using a pressure of 200 MPa for 3 h also at both 850 and 1150ºC. The HIP consolidated alloys were subsequently aged at 1200ºC for times of 48, 96, 144, and 228 h. Both small angle neutron scattering (SANS) and Vicker's micro-hardness (μH) measurements were performed on the as-HIPed and aged specimens. A final alloy designated FCRD-NFA1 was consolidated at ORNL. The powders were first canned and degassed at 400ºC then hot extruded at 850º. After extrusion the alloy was annealed for 1 h at 1000ºC and hot cross-rolled to a ≈ 50% thickness of ≈10 mm. A full microscopic analysis was performed on this alloy including SANS, μH, APT, and TEM. Mechanical testing including fracture, creep, and tensile testing is currently underway.

TEM was performed on FIB lift-out specimens using both FEI Titan 300 kV and FEI T20 200 kV instruments. Grain size measurements and NF size and number density measurements typically used bright field imaging. The NFs were manually counted and the size distribution and number density was measured using image J. The convergent beam techniques were used to measure the foil thickness. Atom probe tomography was performed using a LEAP 3000X HR instrument. All samples were prepared using an FEI Helios FIB using the lift-out method outlined by Thompson [3]. Samples were primarily run in voltage mode, with one sample run in laser mode. All voltage mode samples were at temperatures between 35 and 55 K, 1% evaporation rate, 20-25% voltage pulse, and 200 kHz pulse frequency. The normal green laser energy was ≈ 0.2 nJ, but a test on one sample was performed to assess the effects of very high laser energy of 0.7 nJ. All analysis was performed using the IVAS software. SANS was performed at the NIST Center for Neutron Research in Gaithersburg, MD on the NG-7 30m SANS beamline. A collimated neutron beam with 5±0.3 Å wavelength was scattered by 1 mm x 10 mm x 10 mm samples in a 1.7±0.1 T horizontal magnetic field. The raw SANS data consists of an intensity map, $I(x,y) = I(q,\varphi)$, of the neutron counts on a two-dimensional ^{3}He detector. Here φ is the angle with respect to the magnetic field and q is the scattering vector, which is a function of the scattering half angle, θ, and the neutron wavelength, λ. The 64 cm x 64 cm detector with 0.5 cm X 0.5 cm pixel size was located 1.55 m from the sample and offset by ≈ 20 cm in the horizontal direction to give a higher q range of ≈ 0.05 to 4 nm-1, corresponding to a feature size length scale of 12.6 to 1.6 nm ($d \approx 2\pi/\lambda$). Scattering from a control (Fe-14wt.%Cr-3wt.%W-0.4wt.%Ti), that does not contain Y, was subtracted from the alloy of interest to isolate the NF scattering and the resulting signal was fit to determine average diameter (<d>), number density (N), and volume fraction (f) from the sample using the method given by Alinger et al. [4].

STATUS AND PROGRESS

Milled and annealed powders

The TEM micrograph in Figures 1a shows a bimodal grain structure in the 1150ºC-annealed powder, with a mixture of small grains, <0.5 µm, and larger grains, several µm in size. The FIBed sample was too small for an accurate overall grain size measurement. Figure 1b shows the NF distribution, shown by the small dark spots, with an average diameter (<d>) ≈ 1.5 nm, a number density (N) of ≈ 6.5×10^{23} m^{-3}, and a nominal volume fraction (f) of 0.18%.

Three APT tips from the 850ºC annealed powder were analyzed (≈10 million ions) and five tips were analyzed from the 1150ºC annealed powder (≈34.5 million ions). In all cases, a high NF number density was observed. The average bulk composition for both annealing temperatures is shown in Table 1. The bulk composition for the various annealing temperature were generally similar, except that the 1150ºC anneal had a Y content of 0.044 at.% while the 850ºC anneal was 0.076 at.%. Although the Y was lower in the 1150ºC anneal, the range from 0.044 to 0.076 at.% Y is not unexpected and is consistent with previous studies. The low value of Y may be due to the inhomogeneity of the NF distribution or larger Y precipitates that are not observed by APT due to their small number density and the small sample size. There is also a possibly of undercounting Y ions that are undetected in the atom probe analysis. A small amount of N was observed and indicates that the milling procedure minimized contamination compared to some previous alloys.

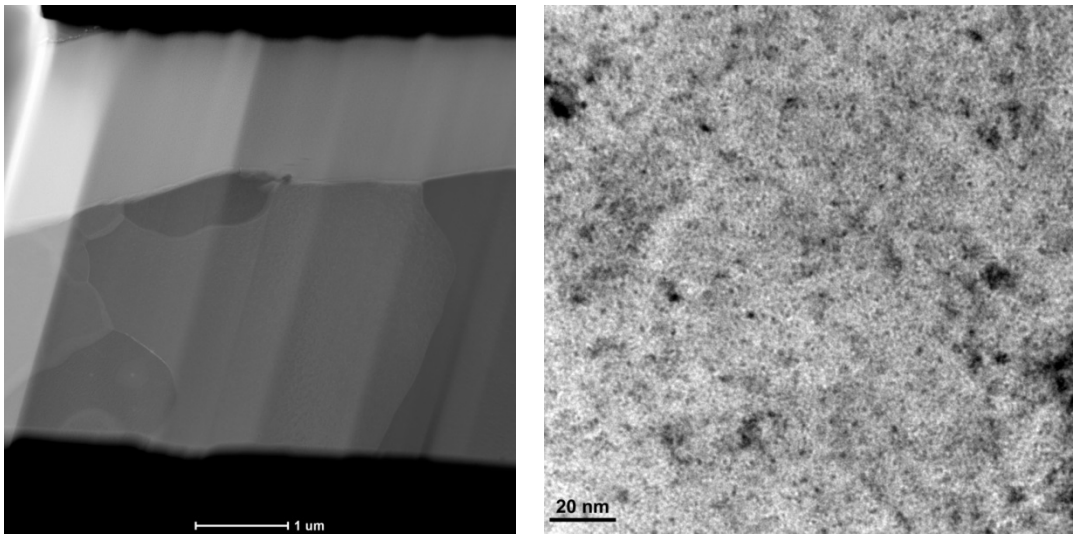

Figure 1. TEM images of 1150ºC annealed powder showing a) bimodal grain size and b) fine dispersion of NF.

Table 1. The average APT bulk composition (at.%) in the V540 850 and 1150ºC annealed powders.

	Fe	Cr	W	Ti	Y	O	C	Si	N
850ºC Anneal	82.61	15.41	0.998	0.381	0.076	0.263	0.064	0.073	0.002
1150ºC Anneal	83.10	15.13	0.980	0.361	0.044	0.225	0.017	0.063	0.002

Table 2 shows the matrix composition, excluding NFs, for the two samples. Again the composition is similar for the two aging temperatures. Except for large reductions in the Ti, Y, and O that are associated with the NFs there is little change between the bulk and matrix compositions. The Ti and O are reduced by ≈ 50% while the Y is reduced by more than 70%.

Table 2. The average APT matrix composition (at.%) in the V540 850 and 1150ºC annealed powders.

	Fe	Cr	W	Ti	Y	O	C	Si	N
850ºC Anneal	83.07	15.38	0.996	0.185	0.018	0.131	0.052	0.066	0.001
1150ºC Anneal	83.482	14.988	0.975	0.241	0.012	0.156	0.013	0.060	0.002

Table 3 shows the average composition of the clusters after correcting for iron and other matrix atoms. Again both alloys show similar average NF composition. There is significant Cr content in the NF of ≈20% and the Y/Ti ratio is ≈ 0.36, typical of other NFAs.

Table 3. The average APT NF composition (at.%) in the V540 850 and 1150ºC annealed powders after removing matrix atoms.

	Cr	W	Ti	Y	O
850ºC Anneal	21.76	0.77	29.24	10.71	34.97
1150ºC Anneal	19.91	0.24	28.99	10.20	38.27

Although the overall average NF composition was similar for the 850ºC and 1150ºC anneals, one 850˚C annealed APT tip showed a population of NFs with Y/Ti ratios > 1. In this particular case, the upper portion of the tip had many NFs that were mostly Y and O as shown in Figure 2. In the bottom 1/3 of the tip, below a possible grain boundary, most of the NF had lower Y/Ti ratios more typical of those found in other NFAs. Since the NFs with higher Y/Ti ratios were only observed in one sample, it is difficult to draw broad conclusions; however, since this alloy was annealed at a lower temperature the NFs may suggest that the Y and O features are present before annealing or cluster first, before reacting with Ti.

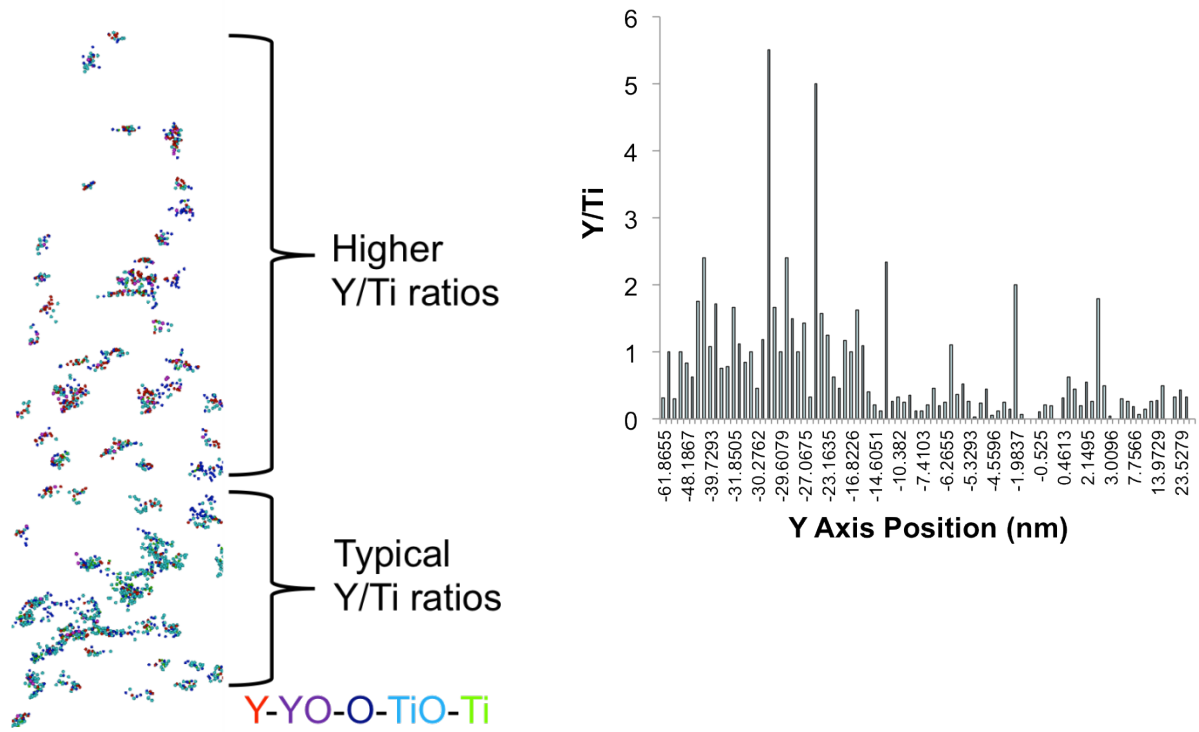

Figure 2. APT analysis on 850ºC sample showing two populations of NF with one set having Y/Ti ratios > 1.

The average NF size (<d>), number density (N), and clustered solute fraction (f_{solute}) for the two powders anneals are shown in Table 4. As expected, the 850ºC anneal had a higher number density and smaller size than the 1150ºC condition. Despite the high Y/Ti ratio found in some NF, in one 850ºC APT tips the overall NF Y/Ti/O ratio was nearly identical.

Table 4. The average NF <d>, N, f and Y/Ti/O ratio measured by APT.

	<d> (nm)	N (10^{23} m^{-3})	f_{solute} (%)	Y/Ti/O
850ºC Anneal	1.8	10.0	0.51	14/39/47
1150ºC Anneal	2.1	4.8	0.38	14/38/48

Figure 3 shows atoms maps of one large precipitate that was found on a grain boundary in the 850ºC annealed powder. This precipitate was composed mainly of Ti, Si, and C with trace amounts of N in the center. No other larger precipitates were observed in either the 850 or 1150ºC tips.

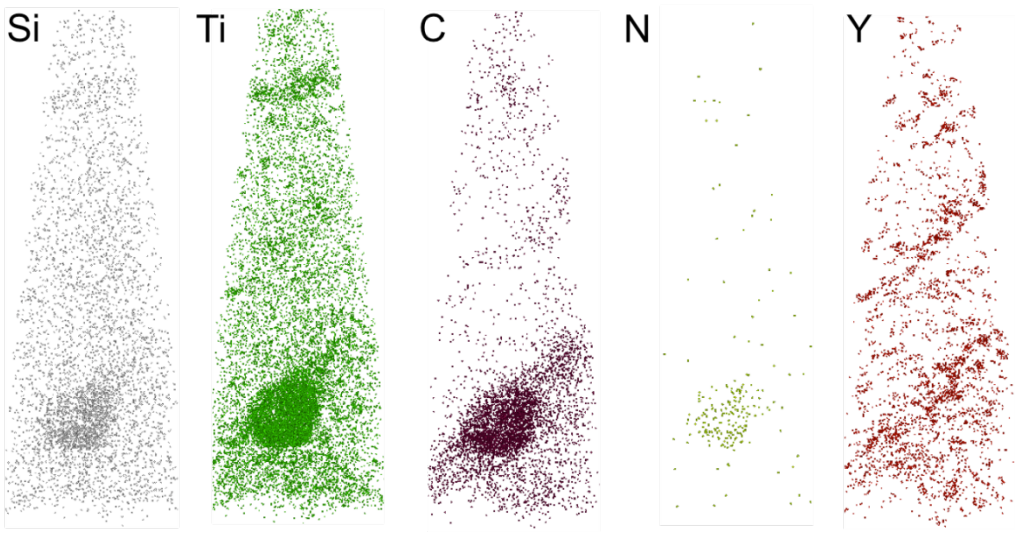

Figure 3. Atom map showing large Ti-Si-C-N precipitate on possible grain boundary in 850ºC annealed powder.

Extruded alloy FCRD-NFA1

The FCRD-NFA1 alloy consolidated by extruding at 850ºC and subsequently cross-rolled to 50% thickness after annealing for 1 h at 1000ºC was analyzed by TEM, APT, and SANS. The microstructure is shown in the TEM images in Figure 4. This alloy showed a unimodal grain size distribution with the average size of ≈ 0.5 µm. This is similar to the previous extruded alloy, PM2 [2].

EDX analysis on some of the larger precipitates showed that they were mainly composed of Ti and N, indicating some contamination may have occurred. An example TEM image showing the larger precipitates on grain boundaries is shown in Figure 5. TEM also showed the presence of the smaller Y-Ti-O NF and measured the <d>, N and f to be 2.1±1.3 nm, 1.6×10^{23} m^{-3}, and 0.25%, respectively. EDX was performed on larger NF from 5 to 20 nm in diameter. The measured Y/Ti ratio in these larger NF ranged from 0.5 to 1.3. SANS analysis was also performed on the FCRD-NFA1 and showed slightly larger NF (3 nm) with higher number density (6.0×10^{23} m^{-3}) and volume fraction (0.82%) compared to the TEM results. Figure 6 compares the 45±15º scattering curves of the FCRD-NFA1 alloy with NFA alloy MA957 and a Fe14Cr control. Overall, the scattering is slightly higher in the FCRD-NFA1 but still comparable to that for MA957.

Almost all the tips FCRD-NFA1 atom probe tips fractured early when encountering large Ti rich precipitates. Figure 7 shows atom maps from one sample with two large precipitates composed mainly of Ti, O, C, and N. Smaller Y-Ti-O NF were found in the rest of the sample. The NF Y/Ti/O ratio for FCRD-NFA1 is 14/42/45 with slightly higher, but still similar compared to the milled and annealed powders. The Y/Ti/Cr/O was 11/32/24/34, again showing high 20% Cr in the NFs. This alloy included a processing step at 1000ºC between the powder temperatures annealing temperature, and the N and <d> fell between the annealed powders at 6.9×10^{23} m^{-3} and 2.02±0.78, respectively. The f was ≈ 0.74%.

The APT bulk and matrix composition from the FCRD-NFA1 sample without large Ti-rich precipitates is shown in Table 5. Again the majority of Y, Ti, and O are found in the precipitates and not in the matrix. This tip also has higher C content compared to the annealed powders

(0.138 at.% vs 0.064 at.%). Part of this C contamination may come from the can used during extrusion, since the APT tip was taken near the sample/can interface.

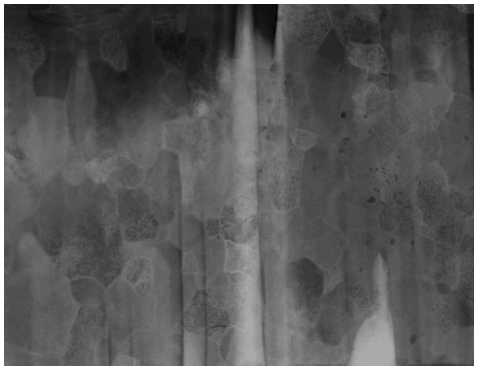

Figure 4. TEM image showing grain structure in FCRD-NFA1 alloy.

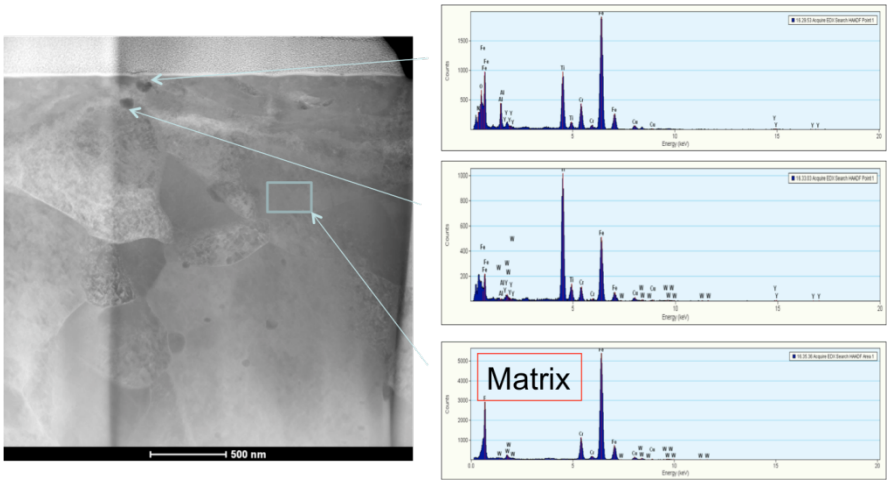

Figure 5. TEM image of the FCRD-NFA1 alloy showing the presence of larger precipitates on grain boundaries that are mainly composed of Ti and N.

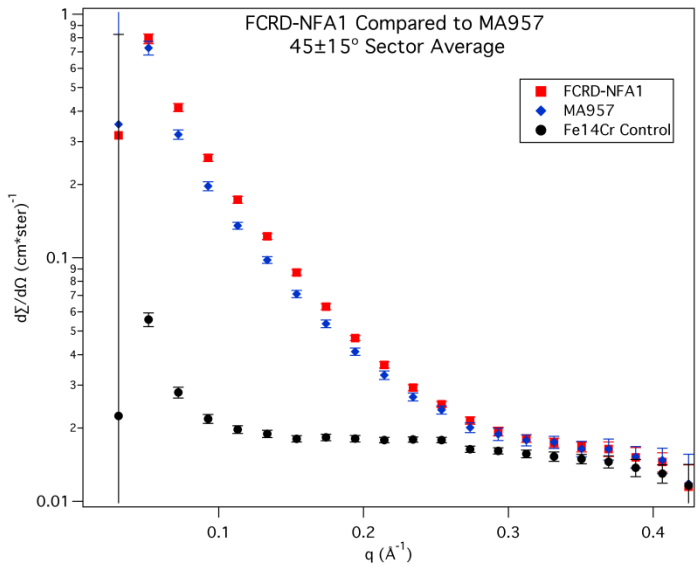

Figure 6. SANS 45º scattering curves comparing FCRD-NFA1, MA957, and Fe14Cr control.

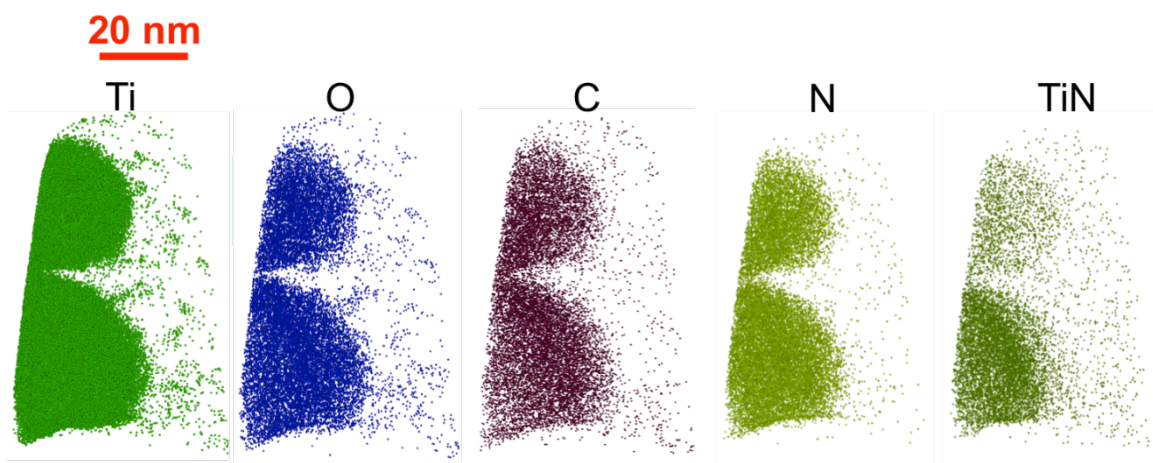

Figure 7. Atom maps showing large precipitates in FCRD-NFA1 composed of Ti, O, C, and N.

Table 5. The APT bulk and matrix composition (at.%) in the FCRD-NFA1 extruded alloy.

	Fe	Cr	W	Ti	Y	O	C	Si	N
Bulk	82.94	15.05	0.967	0.283	0.090	0.366	0.138	0.076	0.006
Matrix	83.57	14.97	0.969	0.056	0.016	0.125	0.127	0.073	0.005

Table 6 compares two previously characterized NFAs with the newest FCRD-NFA1 alloy. Alloy PM2 was the smaller batch precursor to FCRD-NFA1 and MA957 is an older NFA that has been extensively studied. The results from different characterization methods are shown along with the corresponding average <d>, N and f. The APT Y/Ti/O ratio, μH, and grain size are also given. The newer 14YWT NFAs have slightly smaller NFs compared to MA957, but similar number densities and compositions. The microhardness is slightly higher in the newer 14YWT alloys and they have a smaller average grain size. The grains are only slightly elongated in the newer extrusions compared to MA957.

High temperature aging

SANS was performed on the 850 and 1150ºC HIP consolidated alloys as well as aged specimens. All the HIP condition were aged at 1200ºC for 48, 96, 144, and 228 h. Currently only the 48 h aging SANS data has been analyzed. Results from the longer aging times will be reported in the future and will be compared to previous aging performed on MA957. As noted above, the 850ºC HIP baseline alloy had the smallest NF and highest number density at <d> = 2.1 nm and N = 2.93×10^{24} m^{-3}. This corresponded to a nominal NF volume fraction of 1.5% and resulted in a μH of 495±16. The 1150ºC HIP had a <d> = 3.0 nm, N = 7.2×10^{23} m^{-3}, and f = 1.0% resulting in a μH of 357±17. After aging at 1200ºC for 48 h the NF populations in the two conditions were nearly identical. The aged 850ºC HIP had a <d> = 3.6 nm, N = 3.6×10^{23} m^{-3}, and f = 0.90%. The aged 1150ºC HIP had a <d> = 3.7 nm, N = 3.3×10^{23} m^{-3}, and f = 0.9%. The microhardness in the 850 and 1150ºC HIPs after aging were 304±36 and 308±34, respectively. The magnetic to nuclear scattering ratio (M/N) was similar in both alloys at 1.2 for the HIP at 850ºC and 1.1 for the 1150ºC HIP consolidation. This is slightly below the expected value of 1.4 for a population of $Y_2Ti_2O_7$ NF. The M/N in the un-aged alloys is similar to the FCRD-NFA1 alloy with M/N = 1.2. After aging the M/N increased to 1.5 and 1.6 in both cases.

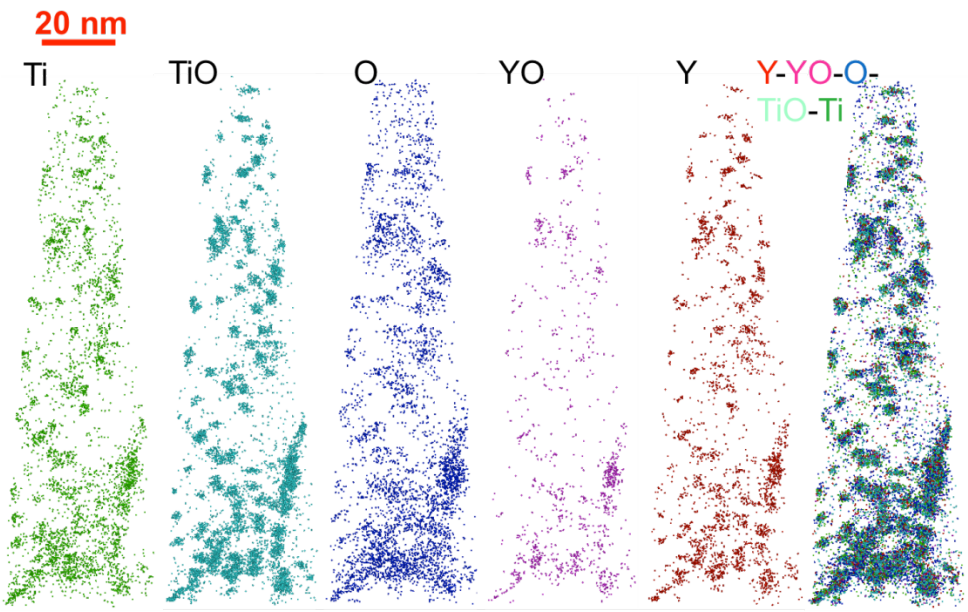

Figure 8. Atom maps showing high number density of Y-Ti-O NF in FCRD-NFA1.

Table 6. Comparison of 14YWT alloys FCRD-NFA1 and PM2 with MA957.

Technique	**NFA1**	**PM2**	**MA957**
TEM <d> (nm)	2.1	1.4	2.8
APT <d> (nm)	2.0	2.1	2.7
SANS <d> (nm)	3.0	2.8	2.7
Average (nm)	2.4	2.1	2.7
TEM N (10^{23} m^{-3})	1.6	5.8	2.6
APT N (10^{23} m^{-3})	6.9	11.0	5.1
SANS N (10^{23} m^{-3})	6.0	8.9	9.0
Average (10^{23} m^{-3})	4.8	8.6	5.6
TEM f (%)	0.25	-	0.40
APT f (%)	0.74	-	0.51
SANS f (%)	0.82	1.00	0.90
Average (%)	0.60	1.00	0.60
APT Y/Ti/O	14/42/45	12/43/40	14/46/40
μH	359±18	401±15	336±8
Grain Size (μm)	454	424	1.47x0.63

Conclusions and future work

The new extruded and cross-rolled FCRD-NFA1 larger heat has a similar microstructure and NF distribution to the previously processed, smaller precursor batch PM2 alloy. In both cases high number densities of Y-Ti-O NFs were observed with a similar character. One notable exception is that there appears to be a greater number of larger, Ti-rich precipitates in the FCRD-NFA1. These larger precipitates were observed both in TEM and APT.

Further comparison between PM2 and FCRD-NFA1 will evaluate the mechanical properties. Limited mechanical property data from PM2 showed promising creep resistance as well as acceptable fracture toughness. The larger volume of FCRD-NFA1 material will allow for a more comprehensive mechanical property investigation. Figure 9 shows the type of samples and orientations that are currently being tested. Fracture testing will occur using one-half-1/3 bend bar specimens in four orientations: L-T, T-L, T-S and L-S. The first letter corresponds to the direction normal to the crack plane in the directions of the length of the specimen, and the second letter corresponds to the crack propagation direction. Two types of tensile specimens were produced. The flat, 0.5 mm thick specimens will be used for tensile testing both at room temperature and at elevated temperature. The round gauge length specimens will be used for creep testing by performing strain-rate jump tests.

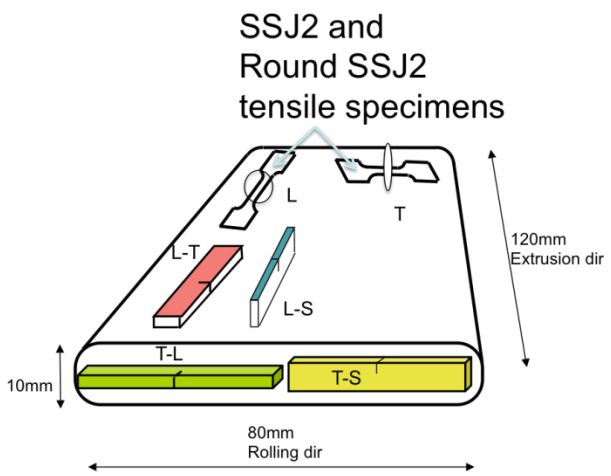

Figure 9. Mechanical test specimen layout in extruded and cross-rolled FCRD-NFA1.

ACKNOWLEDGMENT

This work is part of a multi-laboratory collaboration between LANL, UCSB and ORNL. The research was supported by the DOE Office of Fusion Energy FusMat program, as well as the DOE Office of Nuclear Energy under NEUP grants and by a subcontract from the LANL FCRD program. We acknowledge the support of the National Institute of Standards and Technology, U.S. Department of Commerce, in providing the neutron research facilities used in this work. This work was made possible through use of the Microscopy and Microanalysis facility located at the California Nanosystems Institute (CNSI) at UCSB.

REFERENCES

[1] N. J. Cunningham, "Study of the Structure, Composition, and Stability of Y-Ti-O nm-Scale Features in Nano-Structured Ferritic Alloys," Ph.D. Thesis, University of California, Santa Barbara, Santa Barbara CA (2012).

[2] N. J. Cunningham, Y. Wu, G. R. Odette, D. Gragg, K. Fields, D. T. Hoelzer, and S. A. Maloy, "Characterization of the Final Precursor Alloy to a Larger Best Practice Heat of 14YWT," DOE Fusion Reactor Materials Program Semiannual Progress Report for the Period Ending December 31, 2012, DOE/ER-0313/53.

[3] K. Thompson, D. Lawrence, D. J. Larson, J. D. Olson, T. F. Kelly, and B. Gorman, "In Situ Site-Specific Specimen Preparation for Atom Probe Tomography," *Ultramicroscopy* **107**, 2007, 131.

[4] M. J. Alinger, G. R. Odette, and D. T. Hoelzer, "On the Role of Alloy Composition and Processing Parameters in Nanocluster Formation and Dispersion Strengthening in Nanostructured Ferritic Alloys," *Acta Mater.* **57**, 2009, 392-406.